Revealing the Impact of Molecular Weight on Mixed Conduction in Glycolated Polythiophenes Through Electrolyte Choice

Authors: Joshua Tropp,[a,†] Dilara Meli,[b,†] Ruiheng Wu,[c] Bohan Xu,[b] Samuel B. Hunt,[d] Jason D. Azoulay,[d] Bryan D. Paulsen,[a] Jonathan Rivnay [a]

[a]Department of Biomedical Engineering, Northwestern University, Evanston, Illinois 60208, United States
[b]Department of Materials Science and Engineering, Northwestern University, Evanston, Illinois 60208, United States
[c]Department of Chemistry, Northwestern University, Evanston, Illinois 60208, United States
[d]School of Polymer Science and Engineering, Hattiesburg, Mississippi 39406, United States

ABSTRACT
Developing material design guidelines for organic mixed ionic–electronic conductors (OMIECs) is critical to enable high efficacy mixed transport within bioelectronics. One important feature which has yet to be thoroughly explored is the role of molecular weight on OMIEC performance. In this work, we examined a series of prototypical glycolated polythiophene materials (P3MEEET) with systematically increasing molecular weights within organic electrochemical transistors (OECTs) – a common testbed for investigating mixed transport. We find that there is improved performance beyond an intermediate molecular weight, however, this relationship is electrolyte dependent. Operando analysis suggests that the enhanced mobility at higher molecular weights may be negated by significant swelling when operated in NaCl due to disruption of intercrystallite charge percolation. The role of molecular weight is revealed through operation in KTFSI, as doping occurs through cation expulsion, preventing detrimental swelling and maintaining percolative pathways. These findings demonstrate the importance of both molecular weight and electrolyte composition to enhance the performance of OMIECs.

TOC Image

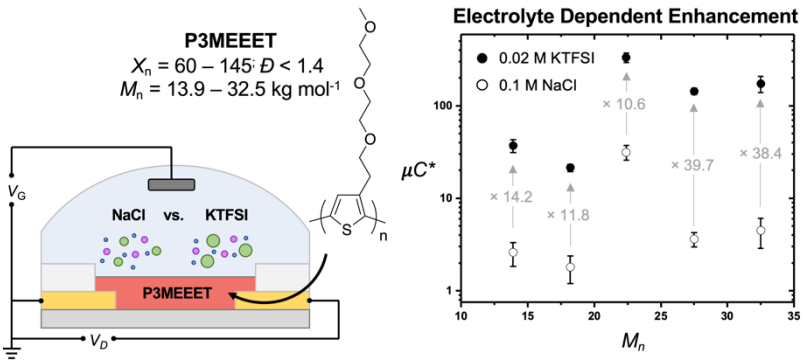

Conjugated polymers (CPs) displaying both electronic and ionic transport have been increasingly deployed in a host of applications including electrochromics, thermoelectrics, and bioelectronics.[1-2] These applications often leverage CP-based organic mixed ionic-electronic conductors (OMIECs) as active materials to couple ionic and electronic signals through charge compensation. In particular, organic electrochemical transistors (OECTs) have shown promise as circuit elements, neuromorphic devices, stimulation elements, and sensors, as the volumetric doping of the OMIEC active material can provide low electrochemical impedance (high capacitance), and thus efficient signal transduction across the biotic/abiotic interface.[3-4] OECTs also provide a convenient platform to investigate the efficacy of mixed conduction within a particular OMIEC,

which is typically quantified by the product of the electronic carrier mobility (μ) and the volumetric capacitance (C^*) given the transconductance (g_m) of the device and the channel dimensions (W = width, L = length, d = film thickness) and operation parameters (V_{th} = threshold voltage, V_G = gate bias).

$$g_m = \frac{Wd}{L}\mu C^*(V_{th} - V_G)$$

Significant efforts have been made to relate the material figure of merit (μC^*) to chemical and morphological features of the OMIEC film to ascertain design guidelines, and therefore enhance performance.[5] Since the initial benchmarking of OMIEC performance for OECTs,[4] research has primarily focused on systematic chemical modifications of the side-chains and polymer backbone to enhance performance.[5-8] While reported μC^* values have dramatically increased through these design strategies, multiple reports of the same material, operated under the same electrolyte environments, display significant variability in performance. For example, high performing p(g2T-TT) has been reported with five different μC^* between ~ 299 and ~ 93 F cm^{-1} V^{-1} s^{-1} in 0.1 M NaCl;[9-13] a similar phenomenon is observed in reports of P3MEEMT.[14-16] This batch-to-batch variability suggests other features of the CP-based OMIEC may play significant roles in mixed conduction.

Conjugated polymers have complexity beyond what their chemical structure would suggest; features including molecular weight distribution, end group chemistry, defects, regioregularity, and metallic impurities have been demonstrated to affect charge transport in other organic electronic devices.[17-21] Of these features, the role of molecular weight distribution has been identified as a key factor dictating electrical, structural, and mechanical properties. For example, in regioregular poly(3-hexylthiophene) (P3HT) higher molecular weight polymers tend to promote charge transport and enhance hole mobility in organic thin-film transistors (OTFTs) through the bridging of crystallites by longer chains, providing connectivity between regions of local order.[17, 22-24] Compared to CP-based active materials within other device architectures, understanding the role of molecular weight on OMIEC performance within an OECT poses a greater challenge due to the interdependent nature of the chemical structure, molecular weight distribution, morphology, and crystallinity on both electronic and ionic transport. Elucidating the impact of molecular weight on mixed transport would not only provide another tool to enhance OMIEC performance but may enable the role of side-chain and backbone modifications to be deconvoluted from varying molecular weight distributions between independently synthesized batches of material.

A thorough understanding of how molecular weight influences mixed transport remains nascent. The most comprehensive study thus far was that of BBL, which demonstrated significant enhancements in both μ and μC^* as the molecular weight increased from 4.9 kDa to 51 kDa.[25] The stronger π-π interactions and higher crystallinity of larger BBL chains led to improved charge transport and therefore performance within the tested OECTs. The relevance of these finding for more common OMIEC motifs, such as polythiophenes, is questionable, since BBL shows high rigidity and volumetric capacitance, and exhibits minimal passive swelling. To address this gap, we investigate regioregular poly(3-[2-(2-methoxyethoxy)ethoxy]ethylthiophene-2,5-diyl) (P3MEEET), a simple prototypical polythiophene-based OMIEC with glycolated side-chains. Kumada catalyst transfer polymerization (KCTP) was used to obtain polymers with molecular weights ranging from 13.9 to 32.5 kg mol^{-1}, or X_n from 60 to 145 (**Figure 1a**) – to our knowledge the high molecular weight batch is the largest reported for a regioregular glycolated polythiophene synthesized via KCTP (**Table S1**). As this range includes the important structural transition from chain-extended crystals to interlinked crystalline lamellae and amorphous regions for P3HT,[17] we

anticipate that a similar relationship between molecular-weight and charge transport would be observed within these chain-lengths for P3MEEET. As OMIECs operate through volumetric ingress of ions, the relationship between OECT performance and molecular weight were investigated within two different prototypical electrolyte compositions, NaCl and KTFSI (**Figure 1b**). We demonstrate that there is a molecular weight dependence on mixed transport within glycolated polythiophenes, however, this relationship is electrolyte dependent. Elevated OMIEC performance was observed beyond an intermediate molecular weight threshold within both the KTSFI and NaCl electrolytes, however, both μC^* and g_m were relatively enhanced in KTSFI compared to NaCl at higher molecular weights, primarily due to a molecular weight-dependent increase in mobility. While ex-situ characterization is a great tool for rapid screening, it's inherently limited to probing material properties in the dry state. OMIECs in particular, experience significant structure modulation upon electrolyte exposure and under electrochemical bias; in-situ and operando characterization techniques allow for analysis conditions better resembling the dynamic behavior of OMIECs within OECTs.[26-27, 36] To that extent, thin films comprising P3MEEET with differing molecular weights were investigated using in-situ grazing-incidence wide-angle X-ray scattering (GIWAXS) and electrochemical quartz crystal microbalance with dissipation monitoring (E-QCMD), to understand the role of electrolyte composition on the molecular weight dependence of mixed conduction. Operando analysis suggested that the enhanced mobility of P3MEEET at higher molecular weights may be negated by significant swelling when operated in NaCl due to disruption of intercrystallite charge percolation. The role of molecular weight was revealed through operation in KTFSI electrolyte, as doping occurs through cation expulsion, preventing the determinantal swelling otherwise observed at higher molecular weights in NaCl, thereby maintaining percolative pathways. The highest performing batch of P3MEEET was at an intermediate molecular weight (M_n = 22.4 kg mol^{-1}) when operated within KTFSI (μC^* = 332 F cm^{-1} V^{-1} s^{-1}), making it the highest performing glycolated polythiophene homopolymeric OMIEC to-date. These findings demonstrate the importance of both molecular weight and electrolyte composition to enhance OECT performance of glycolated polythiophenes.

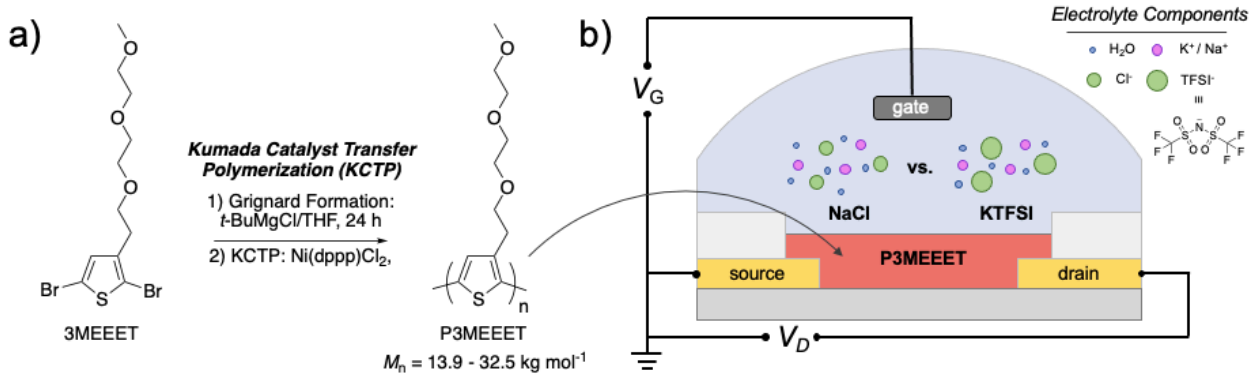

Figure 1. (a) Kumada catalyst transfer polymerization procedure to obtain polymers P3MEEET with varying molecular weight distributions. (b) OECT device schematic displaying P3MEEET as the active layer operated in electrolyte comprising either NaCl or KTFSI.

We chose poly(3-[2-(2-methoxyethoxy)ethoxy]ethylthiophene-2,5-diyl) (P3MEEET) as a model system to investigate the role of molecular weight on mixed transport due to its relatively high-performance, structural simplicity, and accessibility through well-established Kumada catalyst transfer polymerization (KCTP). Synthesis via KCTP is conceptually attractive as the existence of a long-lived π-complex via ring walking enables low dispersity ($Đ = M_n/M_w$) and control over

molecular weight unlike traditional step-growth mediated C-C coupling polymerization processes (Stille, Suzuki). Each P3MEEET batch was polymerized following previously reported procedures using [1,3-bis- (diphenylphosphino)propane]dichloronickel(II) ($NiCl_2$(dppp)) as a catalyst and tert-butyl magnesium chloride as a Grignard reagent (**Figure 1a**).[14] Molecular weight control is enabled in KCTP through modifying [Ni]/$[M]_0$, where higher molecular weight is afforded with lower catalyst loading as there are fewer propagating chains.[28] By systematically lowering the relative loading of catalyst, batches of P3MEEET were synthesized with number average molecular weights (M_n) ranging from 13.9 to 32.5 kg mol^{-1} (**Figure 2a**). Further decreasing the catalyst loading did not produce polymer with higher molecular weight (**Figure S1**); the $Đ \sim 1.4$ for each batch of material suggests incomplete 3MEEET activation, an observed phenomena when polymerizing hygroscopic monomers, leading to premature termination and therefore limited molecular weight.[29-30] Even with these shortcomings, KCTP was used to synthesize multiple batches of P3MEEET with relatively narrow dispersity, well below the Fluory-Shultz distribution afforded by alternative step-growth systems, with systematically increasing M_n in ~ 5 kg mol^{-1} increments from P3MEEET-1 to P3MEEET-5. The molecular weight distributions of each batch were obtained with high resolution as an advanced polymer chromatography (APC) system was utilized (*See Supporting Information*); the unimodal and relatively smooth profile of each batch under high resolution APC indicates a particularly high purity of each batch. The higher molecular weight of P3MEEET-3 – P3MEEET-5 compared to previously reported glycolated polythiophenes synthesized by KCTP (**Table S1**) allowed for the systematic study of molecular weight on performance within an organic electrochemical transistor (OECTs) for this class of material.

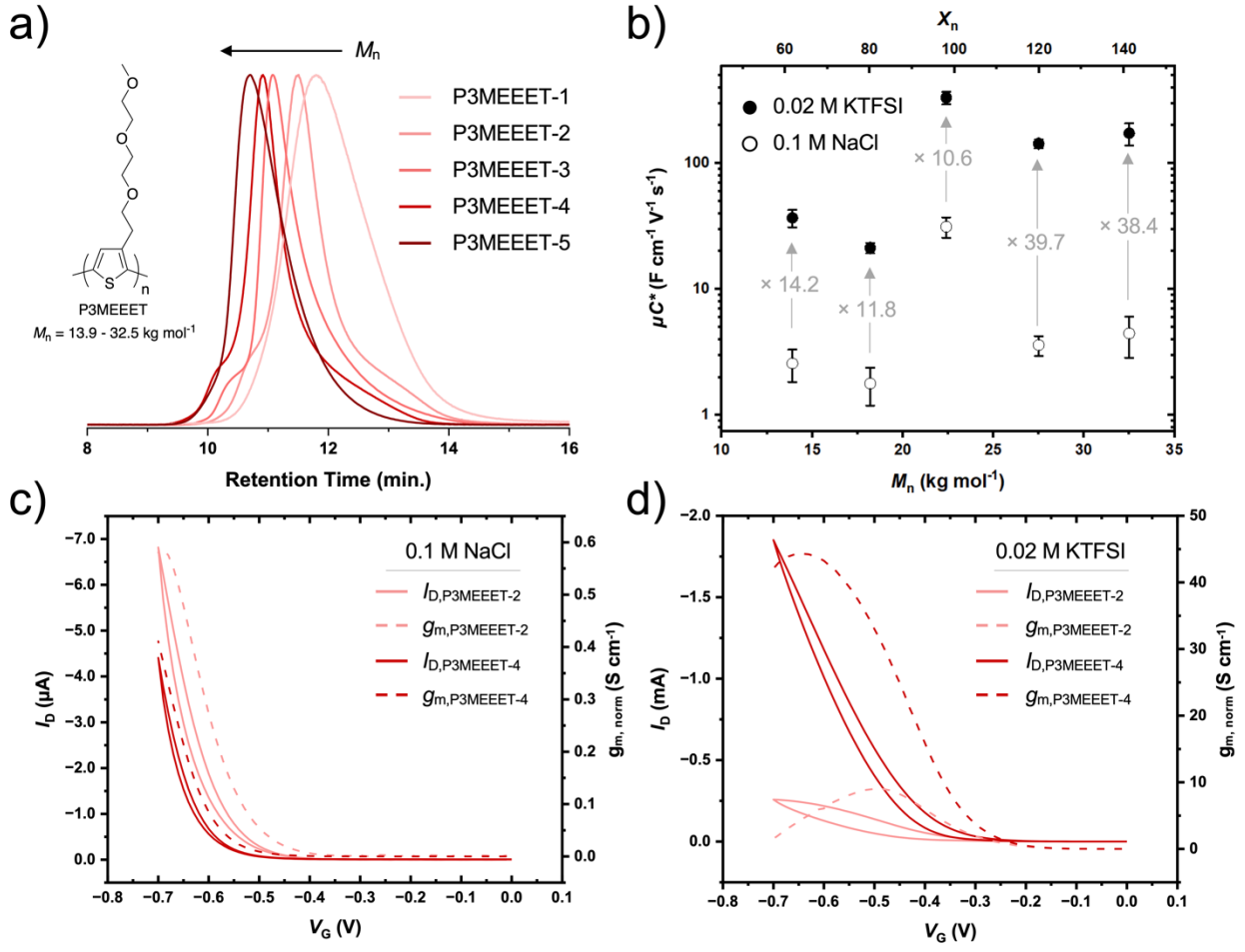

Figure 2. (a) GPC traces of P3MEEET batches of **Table 1**. (b) Comparison of μC^* figure of merit values across the molecular weight series in both 0.02 M KTFSI and 0.1 m NaCl. (c) Representative transfer curves for P3MEEET-2 and P3MEEET-4 at $V_D = V_G$ at 100 mV s^{-1} in 0.1 M NaCl (W = 10 μm, L = 100 μm, and ~140 nm thickness). (d) Representative transfer curves for P3MEEET-2 and P3MEEET-4 at $V_D = V_G$ at 100 mV s^{-1} in 0.02 M KTFSI (W = 10 μm, L = 100 μm, and ~140 nm thickness). Dotted lines show the transconductance in each electrolyte on the right axis.

We first studied the performance of each P3MEEET batch in OECTs operating in conventional 0.1 M NaCl electrolyte (**Figure 2c**, **Table 1**). OECTs operated within NaCl display a slight decrease in threshold voltage ($|V_{th}|$) with increasing molecular weight, consistent with previous reports.[25] The μC^* of P3MEEET shows varies depending on the molecular weight, which is primarily due to variations in μ, as there was no observed relationship between C* with molecular weight (**Figure S2**). In particular, P3MEEET-3 performed significantly better than other materials in the series due to its increased mobility of 0.14 $cm^2 V^{-1} s^{-1}$, indicating that optimal performance is reached at an intermediate molecular weight (**Figure 2b**). Unlike the behavior of polythiophenes in organic field-effect transistors (OFETs) which typically first show enhancements in carrier mobility with increased molecular weight followed by a leveling off at a given threshold,[17] there seems to be an indirect relationship between molecular weight and mobility within an OECT – consistent with a previous report of p(g2T-T).[31] The high μ_{OECT} for P3MEEET-3 is notable as it is significantly (~ 1 - 2 orders of magnitude) larger than other reports of similar glycolated polythiophenes operated within the same electrolyte and is comparable to previously reports of P3MEEET operated in alternative electrolytes (**Table S2**).

Table 1. OECT Parameters and Material Figures of Merit

polymer	M_n (kg mol^{-1})	$Đ$	electrolyte	V_{th}[a] (V)	$g_{m,norm}$[b] (S cm^{-1})	μ_{sat}[a] ($cm^2 V^{-1} s^{-1}$)	C^*[b] (F cm^{-3})	μC^*[c] (F $cm^{-1} V^{-1} s^{-1}$)
P3MEEET-1	13.9	1.38	0.1 M NaCl	-0.50	0.34 ± 0.07	0.02 ± 0.004	153 ± 29	2.6 ± 0.7
P3MEEET-2	18.2	1.36	0.1 M NaCl	-0.50	0.23 ± 0.06	0.02 ± 0.005	80 ± 20	1.8 ± 0.6
P3MEEET-3	22.4	1.31	0.1 M NaCl	-0.54	4.18 ± 0.27	0.14 ± 0.009	219 ± 38	31.4 ± 5.8
P3MEEET-4	27.5	1.35	0.1 M NaCl	-0.56	0.50 ± 0.03	0.02 ± 0.001	192 ± 32	3.6 ± 0.6
P3MEEET-5	32.5	1.26	0.1 M NaCl	-0.63	0.60 ± 0.13	0.02 ± 0.006	171 ± 48	4.5 ± 1.6
P3MEEET-1	13.9	1.38	0.02 M KTFSI	-0.23	3.79 ± 0.51	0.25 ± 0.036	146 ± 10	36.9 ± 5.8
P3MEEET-2	18.2	1.36	0.02 M KTFSI	-0.21	2.21 ± 0.10	0.27 ± 0.007	79 ± 7	21.3 ± 2.0
P3MEEET-3	22.4	1.31	0.02 M KTFSI	-0.19	32.2 ± 1.87	2.14 ± 0.153	156 ± 1	332 ± 37.7
P3MEEET-4	27.5	1.35	0.02 M KTFSI	-0.26	15.8 ± 0.98	1.23 ± 0.070	116 ± 7	143 ± 11.4
-	-	-	- [d]	-0.29	24.6 ± 4.13	1.20 ± 0.201	180 ± 21	216 ± 43.9
P3MEEET-5	32.5	1.26	0.02 M KTFSI	-0.22	15.6 ± 1.14	1.32 ± 0.064	130 ± 25	173 ± 34.2

[a]μ_{sat} OECT saturation mobility and threshold voltage (V_{th}) were extracted from fits of $I_d^{1/2}$ vs. V_G plots. [b]Average volumetric capacitance beyond the V_{th} determined by electrochemical impedance spectroscopy. [c]Maximum transconductance and μC^* extracted from the slope of the saturated transfer curves at V_{th} - 135 mV. The average transconductance values were normalized by the channel geometry. Reported uncertainties are one standard deviation with n = 6 and n = 3 devices for NaCl and KTSFI electrolytes respectively. [d]No previous exposure to NaCl electrolyte.

As the composition of the electrolyte is understood to dramatically impact swelling, charging, and transport of organic mixed conductors,[32] we tested the same OECTs in 0.02 M KTFSI, a prototypical electrolyte with a hydrophobic anion, to further probe the effect of molecular weight. The primary purpose for using the same devices in both electrolytes was to keep experiments as comparable as possible; this was possible due to the comparable performance of the transistors when tested in KTFSI with and without prior exposure to NaCl (**Table 1, P3MEEET-4**). Device

operation in KTFSI displayed lower barriers to hole injection (V_{th} was less negative) for all polymer batches, which can be attributed to the better doping efficiency of KTFSI as compared to NaCl.[33-34] While each batch of material showed an increase in performance when operated in KTFSI, those with lower molecular weights in the series (P3MEEET-1, P3MEET-2, and P3MEET-3) only showed a ~ 10-15-fold increase in μC^*, whereas those with higher molecular weight showed ~ 39-fold increases, suggesting a molecular weight dependent threshold for charge percolation (**Figure 2b**). The C* for each batch were lower when operated in KTFSI than in NaCl, highlighting the observed improvement in μC^* is primarily due to an increase in μ. The best performing polymer in this electrolyte too, remains P3MEEET-3, with a μC^* of 332 F cm^{-1} V^{-1} s^{-1} due to its μ of 2.14 cm^2 V^{-1} s^{-1}, making it the highest performing polythiophene homopolymer OMIEC to-date (**Table S2, Figure S3**), and is on par with some of the best performing p-type materials, with greater structural complexity.[5] To determine if this batch of P3MEEET was an outlier, an independently synthesized batch with similar molecular weight and dispersity was tested, and also demonstrated higher performance than the lower and higher molecular wight batches (**P3MEEET-8**, **Figure S6**).

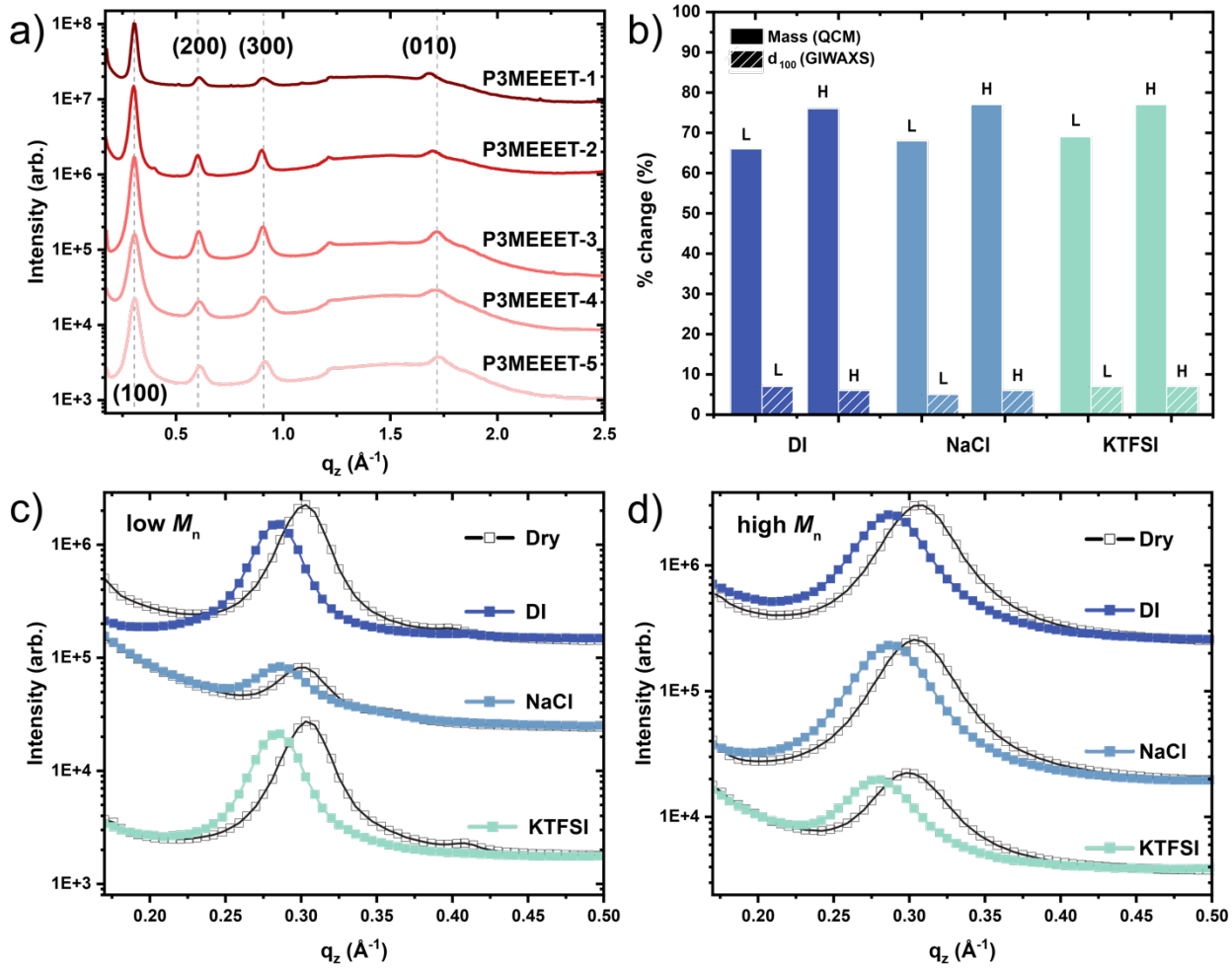

Figure 3. (a) Out-of-plane GIWAXS linecuts of dry P3MEEET films showing three orders of lamellar stacking, labeled (100), (200), and (300), and π stacking, labeled (010). (b) Mass (solid bars) and lamellar spacing (striped bars) changes upon hydration with deionized water (DI), 0.1 M NaCl, or 0.02 M KTFSI of low (L) and high (H) molecular weight films. Lamellar peak shift (100) between dry and exposed films of (c) low and (d) high molecular weights, respectively.

To relate the molecular weight dependence of hole mobility to microscopic structure, ex-situ GIWAXS was performed on drop-cast films of each material. P3MEEET-1 through P3MEEET-5 displayed no significant structural differences in the dry state, though a slight decrease in π-spacing with increasing molecular weight can be observed (**Figure 3a, Table S3**). Each P3MEEET batch showed isotropic π and lamellar scattering which is likely due to the thickness of the samples (**Figure S4**). However, due to poor resolution of the horizon in in-situ GIWAXS experiments (**Figure S4**), we exclusively focus our discussion on out-of-plane features. The polymers demonstrate dry lamellar (100) spacing of ~20.5 - 21 Å and π spacing of ~3.7 Å which are in agreement with previous literature reports.[14] While ex-situ GIWAXS investigations can be informative, since observed differences are due to operation in aqueous media, in-situ and operando characterization are critical.[26] As such, we first investigated passive swelling of the material in deionized (DI) H_2O, 0.1 M NaCl, and 0.02 M KTFSI. We performed in-situ GIWAXS using a custom frit cell mount (**Figure S4a**),[27] and quartz crystal microbalance (EQCM-D) experiments on sample polymers below 20 and above 25 kg mol^{-1}, which in the following discussion will be referred to as "low" and "high" molecular weight, respectively. In-situ GIWAXS shows swelling of the lamellae in all three conditions, where polymers in KTFSI swell slightly more than those in NaCl, as seen in **Figure 3b**. This is corroborated by swelling in EQCM-D experiments however, we observed significantly more swelling of the entire film compared to swelling of the crystallites alone, as seen in the GIWAXS results (**Figure 3b**). Crystallite expansion can only accommodate at most a 16% mass increase due to electrolyte uptake into the crystallite free volume (see SI section 4), compared to a >50% total mass increase as determined by EQCM-D, thus the majority of passive swelling occurs in the amorphous regions of the polymer. Regardless of media, high molecular weight polymers swelled ~ 10% more than their low molecular weight counterparts in QCM experiments. Despite the volumetric expansion of the crystallite, we observed only a small decrease in coherence lengths (**Table S3**) and consistent lamellar peak shapes (**Figure 3c-d**), indicating that crystallite structure was maintained in the swollen state, regardless of electrolyte composition. In summary, passive swelling experiments did not reveal molecular weight dependence that immediately explain the trends seen in OECT performance, indicating that observed phenomena are only unveiled under an applied bias.

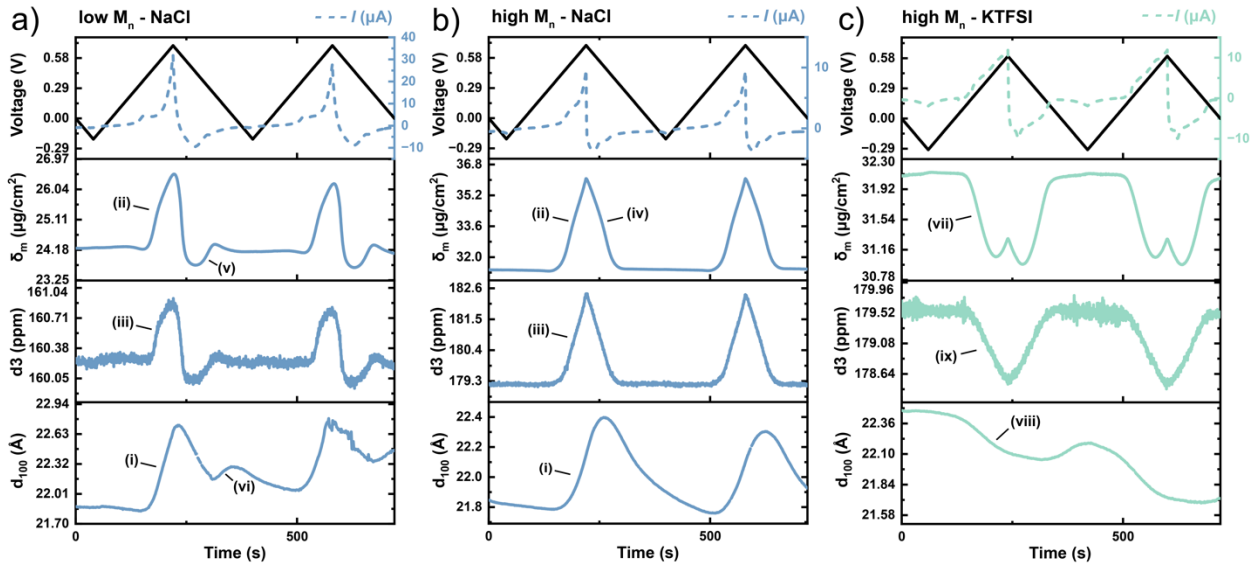

Figure 4. Applied voltage profile (top left), measured current form EQCM-D experiments (top right), measured mass (second row) and dissipation (third row) changes from EQCM-D, and lamellar spacing modulation (bottom row) of (a) low M_n P3MEEET in NaCl, (b) high M_n P3MEEET in NaCl, and (c) high M_n

P3MEEET in KTFSI. Lowercase roman numerals (i)-(ix) are used to aide in understanding processes described in the text with respect to the observed experimental features.

To further investigate the electrolyte-dependent improvement in performance of the higher molecular weight polymers, we performed *operando* GIWAXS and electrochemical quartz crystal microbalance (EQCM-D) experiments on the "low" and "high" molecular weight polymers during electrochemical cycling (**Figure 4**). Lamellar spacing underwent significant modulation upon electrochemical biasing, whereas π-spacing remained largely unchanged in all samples except for high molecular weight samples in KTFSI (*see supporting videos*). Comparing low and high molecular weight polymers in NaCl, it can be deduced that doping occurs via anion uptake in both cases, due to the observable lamellar expansion (i), as well as increases in mass (ii) and dissipation (iii), which agrees with literature.[15, 35] While the overall mass uptake is larger in the high molecular weight polymer, the crystallite volume shows higher modulation in the low molecular weight polymer (**Figure 4a**, **Figure 5**). This suggests that mass uptake in high molecular weight polymers occurs preferentially in the amorphous region. Larger mass modulation within the high molecular weight polymer (**Figure 4b**, **Figure 5**) agrees with the slightly higher volumetric capacitance observed in the OECTs. It's also noteworthy that, while de-doping occurs predominantly via Cl^- expulsion in the high molecular weight polymer (iv), during later stages of the de-doping process (closer to 0 V), low molecular weight polymers show an increase in mass (v), as well as an increase in the lamellar spacing (vi), indicating an uptake of Na^+. In comparison, differences between high and low molecular weight in KTFSI are much more subtle (**Figure 4, Figure S5**). Specifically, the low molecular weight polymer showed smaller modulation of mass, dissipation, and lamellar spacing (**Figure 5**). From the decrease in mass (vii) and lamellar spacing (viii), it can be inferred that doping primarily occurs via cation expulsion, which leads to more "solid-like" polymers, as corroborated by a decrease in dissipation (ix), which could reflect improved hole transport pathways. Enhanced performance of P3MEEET under operation in KTFSI is likely due to doping primarily via cation expulsion rather than anion uptake as in NaCl. During the doping process, polymers in NaCl experience crystalline and amorphous swelling, which is expected to strain percolation, whereas those in KTFSI experience mass expulsion, which improves percolation. The larger modulation of mass for high molecular weight polymers in KTFSI suggests enhanced densification, which may be the source of improved electrochemical performance. The phenomenon of doping via cation expulsion in p-type OECTs has been observed before,[35] and is a direct result of the nature of the electrolyte .[33] We hypothesize that this is particularly pronounced in our materials, since the alkyl spacer near the backbone may improve the ability of the KTFSI anion to reside near the backbone.[33]

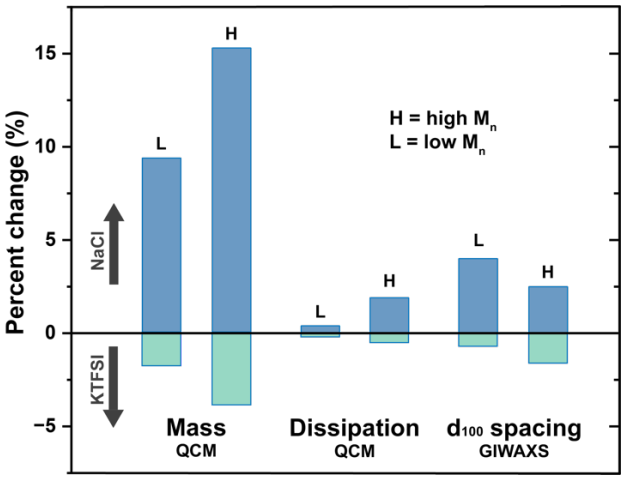

Figure 5. Total modulation of mass, dissipation, and lamellar spacing during doping of low (L) and high (H) molecular weight P3MEEET in NaCl and KTFSI electrolytes.

In conclusion we investigated the relationship between molecular weight and mixed transport in prototypical glycolated polythiophene P3MEEET. When operated within NaCl electrolyte, the batch with intermediate molecular weight P3MEEET-3 was observed to have the optimal μC^* (31.4 F cm^{-1} V^{-1} s^{-1}), with detrimental swelling adversely impacting mixed conduction beyond a molecular weight threshold of 22.4 kg mol^{-1}, obfuscating the otherwise anticipated enhancement in mobility observed in traditional CPs at higher molecular weights. Therefore, to further investigate the influence of molecular weight on mixed conduction, active swelling was regulated through operation within an electrolyte with a more hydrophobic anion ($TFSI^-$). When operated within KTFSI, enhanced μC^* was observed with increasing molecular weight, primarily due to an increase in μ beyond the same threshold observed in NaCl. Through o*perando* GIWAXS and EQCM-D we observed that electrochemical doping of P3MEEET occurred primarily by Cl^- uptake in NaCl, leading to significant swelling at high molecular weights, and K^+ expulsion when operated in KTFSI – both of these behaviors were enhanced at higher molecular weight. Regardless of electrolyte, all polymers experienced significant passive swelling, primarily in the amorphous region, which separated crystalline regions. We hypothesize that this swelling in low molecular weight polymers brought the system to the limit of percolation, whereas in high molecular weight polymers, longer chains were able to maintain connections between crystallites.[23] Since bias-dependent swelling further separated crystallites in NaCl at longer chain lengths, percolation is disrupted, thus counteracting the otherwise beneficial effect of increased molecular weight. In KTFSI, however, doping resulted in an overall contraction of the polymer, improving charge transport pathways in both high and low molecular weight polymers, though low molecular weight polymers remain below the percolation threshold. Therefore, comparisons of both mass and lamellar spacing modulation suggest that the significant improvement of performance at higher molecular weights in KTFSI relative to NaCl is due to (1) the greater expulsion of water leading to denser films, potentially benefiting hole transport and (2) detrimental swelling in NaCl. It is also important to note that other factors may play a role in the varying performance observed between batches at different molecular weights. For example, AFM analysis on low and high molecular weight batches display significant differences in surface roughness, which is one of many factors that can impact volumetric capacitance (**Figure S7**).

The highest performing polymer batch was P3MEEET-3 when operated in KTFSI (μC^* of 332 F cm^{-1} V^{-1} s^{-1}), which showed optimized μ (2.14 cm^2 V^{-1} s^{-1}); a remarkable performance for this class of OMIECs. These results underscore the added complexity of determining molecular design guidelines for mixed conductors which undergo volumetric rather than interfacial electrochemical or electrostatic operation (i.e. EGOFETs or OFETs). The relationship between molecular weight and performance is therefore anticipated to be material dependent, as materials such as P3MEEET display detrimental swelling at higher molecular weights (thus amplifying electrolyte dependence), while other materials which lack side chains such as BBL show minimal passive swelling. This work provides a molecular design strategy to optimize OECT performance for glycolated polythiophenes and offers insight into how such material properties can be investigated and leveraged for other classes of mixed conductors.

Supporting Information

Experimental procedures, tabulated literature comparison of glycolated polythiophene molecular weight and figures of merits for OECTs, tabulated peakfits and coherence length data from ex-situ GIWAXS, a comparison of volumetric capacitance (C^*) of P3MEEET at different molecular weights, scattering patterns from in-situ GIWAXS, AFM images, calculations for free volume estimates, and videos of GIWAXS patterns during electrochemical cycling.

Author Information

Corresponding Authors

Jonathan Rivnay – Department of Biomedical Engineering, Northwestern University, Evanston, Illinois 60208, United States; orcid.org/0000-0002-0602-6485; Email: jrivnay@northwestern.edu

Bryan D. Paulsen – Department of Biomedical Engineering, Northwestern University, Evanston, Illinois 60208, United States; orcid.org/0000-0002-0923-8475; Email: bryan.paulsen@northwestern.edu

Authors

Joshua Tropp – Department of Biomedical Engineering, Northwestern University, Evanston, Illinois 60208, United States; orcid.org/0000-0002-1427-1296

Dilara Meli – Department of Materials Science and Engi neering, Northwestern University, Evanston, Illinois 60208, United States; orcid.org/0000-0002-9032-1697

Ruiheng Wu – Department of Chemistry, Northwestern University, Evanston, Illinois 60208, United States; orcid.org/0000-0003-2666-6110

Bohan Xu – Department of Materials Science and Engineering, Northwestern University, Evanston, Illinois 60208, United States

Samuel B. Hunt – School of Polymer Science and Engineering, Hattiesburg, Mississippi 39406, United States

Jason D. Azoulay – School of Polymer Science and Engineering, Hattiesburg, Mississippi 39406, United States

Author Contributions

† J.T. and D. M. contributed equally to this work.

Acknowledgments

J.R. gratefully acknowledges funding support from Sloan under award no. FG-2019-12046. R.W., B.D.P., and J.R. acknowledge support from the National Science Foundation grant no. NSF DMR-1751308. R.W., D.M. and J.R. acknowledge funding from King Abdullah University of Science and Technology Office of Sponsored Research (OSR) under award no. OSR-2019-CRG8-4086. J.T. was primarily supported by an Office of Naval Research (ONR) Young Investigator Program (YIP) award no. N00014-20-1-2777. This work utilized the Keck-II facility of Northwestern University's NUANCE Center and Northwestern University Micro/Nano Fabrication Facility (NUFAB), which are both partially supported by the Soft and Hybrid Nanotechnology Experimental (SHyNE) Resource (NSF ECCS-1542205), the Materials Research Science and Engineering Center (NSF DMR-1720139), the State of Illinois, and Northwestern University. Additionally, the KeckII facility is partially supported by the International Institute for

Nanotechnology (IIN); the Keck Foundation; and the State of Illinois, through the IIN. Use of the Stanford Synchrotron Radiation Lightsource, SLAC National Accelerator Laboratory, is supported by the U.S. Department of Energy, Office of Science, Office of Basic Energy Sciences under Contract No. DE-AC02-76SF00515. We acknowledge the generous support from Christopher J. Takacs for his assistance with scattering experiments and data analysis.

References

1. Paulsen, B. D.; Tybrandt, K.; Stavrinidou, E.; Rivnay, J., Organic mixed ionic–electronic conductors. *Nat. Mater.* **2020,** *19*, 13-26.
2. Inal, S.; Rivnay, J.; Suiu, A.-O.; Malliaras, G. G.; McCulloch, I., Conjugated Polymers in Bioelectronics. *Acc. Chem. Res.* **2018,** *51*, 1368-1376.
3. Rivnay, J.; Inal, S.; Salleo, A.; Owens, R. M.; Berggren, M.; Malliaras, G. G., Organic electrochemical transistors. *Nat. Rev. Mater.* **2018,** *3*, 17086.
4. Inal, S.; Malliaras, G. G.; Rivnay, J., Benchmarking organic mixed conductors for transistors. *Nat. Commun.* **2017,** *8*, 1767.
5. Paudel, P. R.; Tropp, J.; Kaphle, V.; Azoulay, J. D.; Lüssem, B., Organic electrochemical transistors – from device models to a targeted design of materials. *J. Mater. Chem. C* **2021,** *9*, 9761-9790.
6. Kukhta, N. A.; Marks, A.; Luscombe, C. K., Molecular Design Strategies toward Improvement of Charge Injection and Ionic Conduction in Organic Mixed Ionic–Electronic Conductors for Organic Electrochemical Transistors. *Chem. Rev.* **2022,** *122*, 4325-4355.
7. He, Y.; Kukhta, N. A.; Marks, A.; Luscombe, C. K., The effect of side chain engineering on conjugated polymers in organic electrochemical transistors for bioelectronic applications. *J. Mater. Chem. C* **2022,** *10*, 2314-2332.
8. Li, P.; Lei, T., Molecular design strategies for high-performance organic electrochemical transistors. *J. Polym. Sci.* **2022,** *60*, 377-392.
9. Giovannitti, A.; Sbircea, D.-T.; Inal, S.; Nielsen, C. B.; Bandiello, E.; Hanifi, D. A.; Sessolo, M.; Malliaras, G. G.; McCulloch, I.; Rivnay, J., Controlling the mode of operation of organic transistors through side-chain engineering. *Proc. Natl. Acad. Sci. U.S.A.* **2016,** *113*, 12017-12022.
10. Savva, A.; Cendra, C.; Giugni, A.; Torre, B.; Surgailis, J.; Ohayon, D.; Giovannitti, A.; McCulloch, I.; Di Fabrizio, E.; Salleo, A.; Rivnay, J.; Inal, S., Influence of Water on the Performance of Organic Electrochemical Transistors. *Chem. Mater.* **2019,** *31*, 927-937.
11. Savva, A.; Hallani, R.; Cendra, C.; Surgailis, J.; Hidalgo, T. C.; Wustoni, S.; Sheelamanthula, R.; Chen, X.; Kirkus, M.; Giovannitti, A.; Salleo, A.; McCulloch, I.; Inal, S., Balancing Ionic and Electronic Conduction for High-Performance Organic Electrochemical Transistors. *Adv. Funct. Mater.* **2020,** *30*, 1907657.
12. Moser, M.; Wang, Y.; Hidalgo, T. C.; Liao, H.; Yu, Y.; Chen, J.; Duan, J.; Moruzzi, F.; Griggs, S.; Marks, A.; Gasparini, N.; Wadsworth, A.; Inal, S.; McCulloch, I.; Yue, W., Propylene and butylene glycol: new alternatives to ethylene glycol in conjugated polymers for bioelectronic applications. *Mater. Horiz.* **2022,** *9*, 973-980.

13. Hallani, R. K.; Paulsen, B. D.; Petty, A. J.; Sheelamanthula, R.; Moser, M.; Thorley, K. J.; Sohn, W.; Rashid, R. B.; Savva, A.; Moro, S.; Parker, J. P.; Drury, O.; Alsufyani, M.; Neophytou, M.; Kosco, J.; Inal, S.; Costantini, G.; Rivnay, J.; McCulloch, I., Regiochemistry-Driven Organic Electrochemical Transistor Performance Enhancement in Ethylene Glycol-Functionalized Polythiophenes. *J. Am. Chem. Soc.* **2021,** *143*, 11007-11018.
14. Schmode, P.; Savva, A.; Kahl, R.; Ohayon, D.; Meichsner, F.; Dolynchuk, O.; Thurn-Albrecht, T.; Inal, S.; Thelakkat, M., The Key Role of Side Chain Linkage in Structure Formation and Mixed Conduction of Ethylene Glycol Substituted Polythiophenes. *ACS Appl. Mater. Interfaces* **2020,** *12*, 13029-13039.
15. Flagg, L. Q.; Bischak, C. G.; Onorato, J. W.; Rashid, R. B.; Luscombe, C. K.; Ginger, D. S., Polymer Crystallinity Controls Water Uptake in Glycol Side-Chain Polymer Organic Electrochemical Transistors. *J. Am. Chem. Soc.* **2019,** *141*, 4345-4354.
16. Chen, S. E.; Flagg, L. Q.; Onorato, J. W.; Richter, L. J.; Guo, J.; Luscombe, C. K.; Ginger, D. S., Impact of varying side chain structure on organic electrochemical transistor performance: a series of oligoethylene glycol-substituted polythiophenes. *J. Mater. Chem. A* **2022,** *10*, 10738-10749.
17. Koch, F. P. V.; Rivnay, J.; Foster, S.; Müller, C.; Downing, J. M.; Buchaca-Domingo, E.; Westacott, P.; Yu, L.; Yuan, M.; Baklar, M.; Fei, Z.; Luscombe, C.; McLachlan, M. A.; Heeney, M.; Rumbles, G.; Silva, C.; Salleo, A.; Nelson, J.; Smith, P.; Stingelin, N., The impact of molecular weight on microstructure and charge transport in semicrystalline polymer semiconductors–poly(3-hexylthiophene), a model study. *Prog. Polym. Sci.* **2013,** *38*, 1978-1989.
18. Usluer, Ö.; Abbas, M.; Wantz, G.; Vignau, L.; Hirsch, L.; Grana, E.; Brochon, C.; Cloutet, E.; Hadziioannou, G., Metal Residues in Semiconducting Polymers: Impact on the Performance of Organic Electronic Devices. *ACS Macro Lett.* **2014,** *3*, 1134-1138.
19. Peng, Z.; Ye, L.; Ade, H., Understanding, quantifying, and controlling the molecular ordering of semiconducting polymers: from novices to experts and amorphous to perfect crystals. *Mater. Horiz.* **2022,** *9*, 577-606.
20. Gu, K.; Loo, Y.-L., The Polymer Physics of Multiscale Charge Transport in Conjugated Systems. *J. Polym. Sci. Part B: Polym. Phys.* **2019,** *57*, 1559-1571.
21. Ying, L.; Huang, F.; Bazan, G. C., Regioregular narrow-bandgap-conjugated polymers for plastic electronics. *Nat. Commun.* **2017,** *8*, 14047.
22. Kline, R. J.; McGehee, M. D.; Kadnikova, E. N.; Liu, J.; Fréchet, J. M. J., Controlling the Field-Effect Mobility of Regioregular Polythiophene by Changing the Molecular Weight. *Adv. Mater.* **2003,** *15*, 1519-1522.
23. Noriega, R.; Rivnay, J.; Vandewal, K.; Koch, F. P. V.; Stingelin, N.; Smith, P.; Toney, M. F.; Salleo, A., A general relationship between disorder, aggregation and charge transport in conjugated polymers. *Nat. Mater.* **2013,** *12*, 1038-1044.
24. Kline, R. J.; McGehee, M. D.; Kadnikova, E. N.; Liu, J.; Fréchet, J. M. J.; Toney, M. F., Dependence of Regioregular Poly(3-hexylthiophene) Film Morphology and Field-Effect Mobility on Molecular Weight. *Macromolecules* **2005,** *38*, 3312-3319.
25. Wu, H.-Y.; Yang, C.-Y.; Li, Q.; Kolhe, N. B.; Strakosas, X.; Stoeckel, M.-A.; Wu, Z.; Jin, W.; Savvakis, M.; Kroon, R.; Tu, D.; Woo, H. Y.; Berggren, M.; Jenekhe, S. A.; Fabiano, S., Influence of Molecular Weight on the Organic Electrochemical Transistor Performance of Ladder-Type Conjugated Polymers. *Adv. Mater.* **2022,** *34*, 2106235.

26. Wu, R.; Matta, M.; Paulsen, B. D.; Rivnay, J., Operando Characterization of Organic Mixed Ionic/Electronic Conducting Materials. *Chem. Rev.* **2022,** *122*, 4493-4551.
27. Paulsen, B. D.; Giovannitti, A.; Wu, R.; Strzalka, J.; Zhang, Q.; Rivnay, J.; Takacs, C. J., Electrochemistry of Thin Films with In Situ/Operando Grazing Incidence X-Ray Scattering: Bypassing Electrolyte Scattering for High Fidelity Time Resolved Studies. *Small* **2021,** *17*, 2103213.
28. Bryan, Z. J.; McNeil, A. J., Conjugated Polymer Synthesis via Catalyst-Transfer Polycondensation (CTP): Mechanism, Scope, and Applications. *Macromolecules* **2013,** *46*, 8395-8405.
29. Cheng, S.; Ye, S.; Apte, C. N.; Yudin, A. K.; Seferos, D. S., Improving the Kumada Catalyst Transfer Polymerization with Water-Scavenging Grignard Reagents. *ACS Macro Lett.* **2021,** *10*, 697-701.
30. Song, I. Y.; Kim, J.; Im, M. J.; Moon, B. J.; Park, T., Synthesis and Self-Assembly of Thiophene-Based All-Conjugated Amphiphilic Diblock Copolymers with a Narrow Molecular Weight Distribution. *Macromolecules* **2012,** *45*, 5058-5068.
31. Dai, Y.; Dai, S.; Li, N.; Li, Y.; Moser, M.; Strzalka, J.; Prominski, A.; Liu, Y.; Zhang, Q.; Li, S.; Hu, H.; Liu, W.; Chatterji, S.; Cheng, P.; Tian, B.; McCulloch, I.; Xu, J.; Wang, S., Stretchable Redox-Active Semiconducting Polymers for High-Performance Organic Electrochemical Transistors. *Adv. Mater.* **2022,** *34*, 2201178.
32. Cendra, C.; Giovannitti, A.; Savva, A.; Venkatraman, V.; McCulloch, I.; Salleo, A.; Inal, S.; Rivnay, J., Role of the Anion on the Transport and Structure of Organic Mixed Conductors. *Adv. Funct. Mater.* **2019,** *29*, 1807034.
33. Matta, M.; Wu, R.; Paulsen, B. D.; Petty, A. J.; Sheelamanthula, R.; McCulloch, I.; Schatz, G. C.; Rivnay, J., Ion Coordination and Chelation in a Glycolated Polymer Semiconductor: Molecular Dynamics and X-ray Fluorescence Study. *Chem. Mater.* **2020,** *32* (17), 7301-7308.
34. Wagner, J.; Song, Y.; Lee, T.; Katz, H. E., The combined influence of polythiophene side chains and electrolyte anions on organic electrochemical transistors. *Electrochem Sci Adv.* **2021,** *00*, e2100165.
35. Flagg, L. Q.; Bischak, C. G.; Quezada, R. J.; Onorato, J. W.; Luscombe, C. K.; Ginger, D. S., P-Type Electrochemical Doping Can Occur by Cation Expulsion in a High-Performing Polymer for Organic Electrochemical Transistors. *ACS Materials Lett.* **2020,** *2*, 254-260.
36. Guo, J.; Flagg, L. Q.; Tran, D. K.; Chen, S. E.; Li, R.; Kolhe, N. B.; Giridharagopal, R.; Jenekhe, S. A.; Richter, L. J.; Ginger, D. S., Hydration of a Side-Chain-Free n-Type Semiconducting Ladder Polymer Driven by Electrochemical Doping. *J. Am. Chem. Soc.* **2023,** *145*, 1866-1876.